

Magnetic phase structure of Mn-doped III-V semiconductor quantum wells

H. J. Kim and K. S. Yi*

Department of Physics, Pusan National University, Pusan 609-735, Korea

(Received 3 September 2001; revised manuscript received 15 January 2002; published 8 May 2002)

We present a self-consistent calculation of magnetic phase structure in modulation-doped dilute magnetic III-V semiconductor quantum wells. The spin-split subband structure is calculated at finite temperature and magnetic-field effects on the carrier-induced magnetism are examined in a weak-field regime. The exchange correlation of free carriers is shown to enhance the ferromagnetic tendency. And the temperature T_{th} , below which the system spontaneously becomes fully spin polarized, increases as the doping concentration N_a in nonmagnetic barriers increases. Hysteresis loop of the magnetic quantum well predicts that the remnant magnetization is enhanced as one increases the modulation-doped acceptor impurity concentration.

DOI: 10.1103/PhysRevB.65.193310

PACS number(s): 73.21.Fg, 73.22.Gk, 72.25.-b

I. INTRODUCTION

The interplay between the effects of quantum confinement and the collective magnetic ordering in a dilute magnetic semiconductor (DMS) quantum well (QW) has renewed the interest in both basic and applied research.^{1,2} By spatial modulation of the doping profile and magnetic impurity concentration, DMS quantum structures can lead to a spin-polarized many-particle system.³⁻⁶ This would consist of n_σ electrons of majority spin σ (\downarrow) and $n_{\bar{\sigma}}$ electrons of minority spin $\bar{\sigma}$ (\uparrow) per unit area and show a variety of unique properties which are absent in conventional nonmagnetic structures. The effect of an additional degree of freedom associated with the exchange coupling of itinerant carriers and magnetic impurities in the DMS QW can be varied at finite temperatures.

In this work, we investigate the magnetic phase structures of Mn-doped III-V DMS QW's with an emphasis on the control of the magnetic phase structure of the system in terms of various QW parameters. Our formulation is based on a simple two-band model for the valence band in III-V semiconductors. We limit our considerations to a narrow quasi-two-dimensional DMS quantum well structure, in which the spin-orbit splitting is sufficiently large and the free-carrier concentration is not so high that only the heavy-hole subbands are occupied by the carriers. Present model would readily be extended to a more realistic cases including spin-fluctuation effects and the effects of magnetic anisotropy and band coupling by employing four- or six-band Kohn-Luttinger models for the multiple manifold of the valence band.

II. SELF-CONSISTENT MODEL

We consider a symmetrically modulation-doped QW of a type AlGaAs/Ga_{1-x}Mn_xAs/AlGaAs grown in the $\langle 001 \rangle$ direction, and analyze the electronic structures based on a self-consistent spin-split two-band model of the spin-polarized DMS QW's.⁷ The effects of exchange and correlations of free carriers are included by employing a spin-dependent exchange-correlation potential $v_{xc}^\sigma(z; \zeta)$.⁸ The free-carrier Hartree potential v_H and the electrostatic potential v_s are determined self-consistently by solving the Schrödinger

equation together with the Poisson equation for $v_H(z) + v_s(z)$. Here, the free carriers (holes) in the QW originate from the modulation-doped ionized impurities in nonmagnetic barriers and also in part from the manganese ions localized in the well. Therefore, in our calculation, the potential v_s includes contributions both of modulation-doped ionized impurities of concentration N_a in nonmagnetic barriers and of the magnetic ions of concentration N_{Mn} substituted randomly in the well, in addition to that of the QW band offset V_0 .⁷

In a mean-field approximation,^{9,10} the kinetic exchange interaction $J_{pd}(\vec{r} - \vec{R})$ of free carriers at \vec{r} with d electrons on Mn^{2+} ions of spin $S = 5/2$ localized at \vec{R} is given by

$$H_x = \sigma_y \langle S_y \rangle x \sum_{R_i} J^{sp-d}(\vec{r} - \vec{R}_i), \quad (1)$$

where x is the fraction occupancy of cation sites by magnetic ions and \vec{R}_i denotes the coordinate of the cation sublattice. Here the summation extends over all cation sites. And, hence, the spin-dependent part of the energy of a free carrier is written by⁷

$$V_B^\sigma = \sigma_y [g^* \mu_B B - N_0 \beta x \langle S_y \rangle], \quad (2)$$

where N_0 is the number of cation sites per unit volume. The second term in V_B^σ describes the exchange interaction between the free carrier of spin $\vec{\sigma}$ and Mn^{2+} ions of spin \vec{S} with $\beta = (1/\Omega) \langle \phi | J_{pd} | \phi \rangle$, the expectation value of the exchange coupling integral J_{pd} over a unit cell Ω using the free-carrier Bloch states $|\phi\rangle$.

The spin-polarized QW is described in terms of two spin-subband ladders with eigenvalues $\varepsilon_{i\sigma}(\vec{k})$ and eigenfunctions $|i\vec{k}\sigma\rangle = e^{i\vec{k}\cdot\vec{r}} |i\sigma\rangle$ where i and σ stand for the subband and spin indices, respectively, and \vec{k} the wave vector parallel to the layer. $|i\sigma\rangle = \psi_i^\sigma(z) \chi_\sigma$ is the product of an envelope function $\psi_i^\sigma(z)$ and a spin eigenfunction χ_σ . We confine our consideration to a magnetic QW of width L under an in-plane magnetic field B applied in the y direction parallel to the interface.¹¹ The wave function $\psi_i^\sigma(z)$ is determined by

$$\left[-\frac{\hbar^2}{2m^*} \frac{d^2}{dz^2} + \frac{m^* \omega_c^2}{2} (z - z_0)^2 + v_{s.c.}^\sigma(z) \right] \psi_i^\sigma(z) = E_{ik_x}^\sigma \psi_i^\sigma(z). \quad (3)$$

Here $\omega_c = eB/m^*$, $z_0 = -k_x l_B^2$ with $l_B = \sqrt{\hbar/eB}$, $v_{s.c.}^\sigma(z) = v_H(z) + v_s(z) + V_B^\sigma + v_{xc}^\sigma(z; \zeta)$, and σ ($= \downarrow, \uparrow$) indicates two different spin states. Temperature effect is included by employing the spin-dependent Fermi distribution function

$$f(\epsilon, T) = \frac{1}{\exp\left(\frac{\epsilon - \mu + E_i^\sigma}{k_B T} + 1\right)}$$

in obtaining $v_{s.c.}^\sigma(z)$. In the present work the chemical potential μ is taken to be pinned at the impurity level. We note that a parabolic magnetic confinement induced by in-plane magnetic field makes the solution $\{E_{ik_x}^\sigma; \psi_i^\sigma(z)\}$ k_x dependent, in general. However, in a weak-field regime ($l_B \gg L$), one can neglect the effect of the additional magnetic confinement in a narrow QW, because the second term in Eq. (3) reduces to $\hbar^2 k_x^2 / 2m^*$, leading us to the parabolic k_x dependence of the solution.¹¹ The magnetic field strengths of 1 T $\leq B \leq$ 3 T correspond to the magnetic lengths 25.7 nm $\geq l_B \geq$ 14.8 nm, and we limit ourselves to the weak-field regime ($l_B \gg L$) in the rest of this work. In this regime, the degree of spin polarization of the DMS QW structure could be tuned from the paramagnetic $\zeta = 0$ to the fully polarized ferromagnetic $\zeta = 1$ without any dramatic effect on the orbital motion of the electrons.⁷ Here, the spin polarization ζ is defined by $\zeta = (n_\sigma - n_{\bar{\sigma}}) / n_{2D}$ where $n_{2D} = n_\sigma + n_{\bar{\sigma}}$ the free-carrier two-dimensional (2D) concentration.

The thermal average $\langle S_y \rangle$ taken over all Mn^{2+} ions is given by $\langle S_y \rangle = -\frac{5}{2} B_{5/2}(\xi)$ where $B_{5/2}(\xi)$ is the standard Brillouin function¹² and

$$\xi = \frac{g_{\text{Mn}} \mu_B S B + J_{pd} S \frac{n_{2D} \zeta}{2L}}{k_B T},$$

with $S = 5/2$. The second term in ξ denotes the contribution of the kinetic exchange coupling to the spontaneous magnetization and it takes the feedback mechanism of the magnetization into account.^{2,9} By combining Eq. (3) and the Poisson equation mentioned above, one can obtain the self-consistent subband structure $\{E_i^\sigma, \psi_i^\sigma(z)\}$ at finite temperature.

The subband carrier concentrations and subband energies $\{n_i^\sigma; E_i^\sigma\}$ were obtained by solving Eq. (3) numerically for various magnitudes of magnetic field B at finite temperatures. We employed variational subband wave functions $\psi_i^\sigma(z)$,⁷ and the final solution for a given temperature was obtained by minimizing the total free-carrier energy $E(\zeta)$:

$$E(\zeta) = \sum_{i\sigma} n_i^\sigma \hat{E}_i^\sigma + T(\zeta). \quad (4)$$

Here T denotes the contribution of the two-dimensional kinetic energy parallel to the QW interface and is defined by

$$T(\zeta) = \frac{m^*}{2\pi\hbar^2} \int_0^\infty d\epsilon \epsilon f(\epsilon, T).$$

In Eq. (4), \hat{E}_i^σ indicates the following:

$$\hat{E}_i^\sigma = E_i^\sigma - \frac{1}{2} \langle v_H(z) \rangle, \quad (5)$$

which is needed in order to avoid double counting of the Hartree interaction energy in evaluation of the total energy $E(\zeta)$.

III. RESULT AND DISCUSSION

The carrier spin polarization ζ for a given set of quantum well parameters can be evaluated with the use of the subband structure $\{n_i^\sigma; E_i^\sigma\}$ obtained by solving Eq. (3) and examining spin-split subband carrier concentrations $\{n_i^\sigma\}$ for various values of magnetic field and temperature. Our numerical result shows that, as the magnetic field increases, the quantum well depth of spin-down (majority-spin) electrons becomes deeper through the exchange interaction with Mn^{2+} ions (V_H^σ) and finally saturates to a constant value. As the temperature increases, the concentration of majority-spin electrons n_i^\downarrow is decreased but that of minority-spin electrons n_i^\uparrow is increased until the system becomes paramagnetic. Our calculation shows that the degree of spin polarization in the DMS QW depends strongly on temperature T , free-carrier density n_{2D} , and geometric and doping profile parameters such as well depth V_0 , width L , N_a , and N_{Mn} of the QW. As one increases the degree of spin polarization ζ , i.e., the *effective* magnetic field B , the spin-split subband separation increases, and the free-carrier density n_{2D} in the quantum well increases steadily at high temperatures but increases more rapidly at low temperatures.

In order to obtain the magnetic phase structure of the system in terms of the magnetic field and temperature, the degree of spin polarization is analyzed by varying the magnitudes of an external magnetic field and temperature. A self-consistent magnetic phase diagram of a modulation-doped DMS QW is shown in Fig. 1. We displayed the spin-polarization ζ as functions of temperature and magnetic field. In the region of $0 \leq \zeta < 1$ there exist free carriers in both spin states, whereas the region of $\zeta = 1$ corresponds to the fully spin polarized phase, where all the minority spin subbands are emptied. We could clearly observe that the system shows spontaneous ferromagnetic phase ($\zeta > 0$) below 65 K and becomes fully polarized ferromagnetic phase below about 30 K for the DMS QW of the parameters taken in the figure. The threshold temperature T_{th} below which the system becomes fully polarized ferromagnetic phase ($\zeta = 1$) even in the absence of an external field increases as the doping concentration N_a in nonmagnetic barriers increases. If one neglected the feedback mechanism of the magnetization in obtaining the thermal average $\langle S_y \rangle$ in Eq. (2), the spontaneous spin polarization phase ($\zeta > 0$) would disappear in the ab-

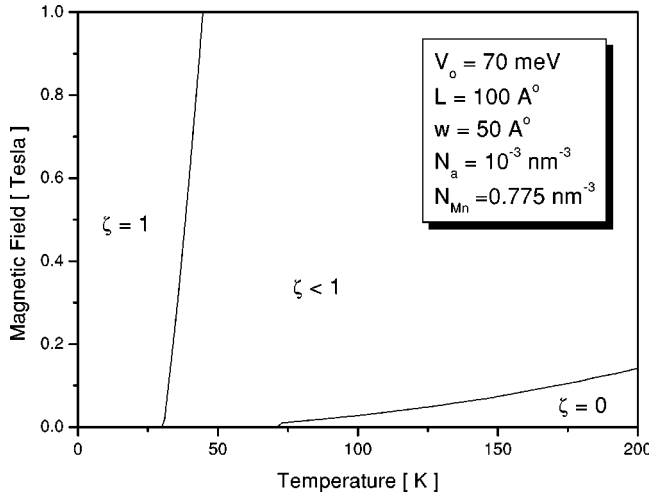


FIG. 1. Magnetic phase diagram of a modulation-doped DMS QW in terms of the temperature and external magnetic field. The value of ζ indicates the degree of spin polarization in each regime.

sence of an external magnetic field. In the figure, w is the width of the spacer layer of the symmetric QW structure.⁷ In numerical calculations, $x=0.035$, $m^*=0.5m_e$, and the coupling strength $J_{pd}=0.15$ eV nm³ for p -type Ga_{1-x}Mn_xAs were taken, and 0.1% of the manganese ions are assumed to contribute to the free carriers (holes) in the well.

The kinetic exchange interaction of free carriers with localized magnetic ions induces the Curie-Weiss transition in the quasi-two-dimensional DMS quantum well. We examined the ferromagnetic ($\zeta \neq 0$) to paramagnetic ($\zeta = 0$) phase transition temperature T_c in terms of the 2D carrier concentration n_{2D} . Figure 2 shows a 2D carrier-concentration dependence of T_c obtained in a local spin-density (LSD) functional and the Hartree calculations. The present self-consistent calculation shows that the exchange correlation of free carriers enhances the ferromagnetic tendency by 10%–

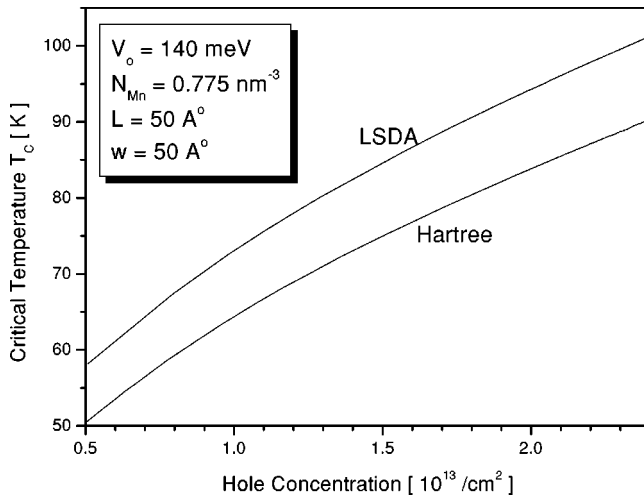


FIG. 2. Two-dimensional carrier-concentration dependence of the ferromagnetic–paramagnetic phase transition temperature T_c obtained in a local spin-density (LSD) functional and Hartree approximations.

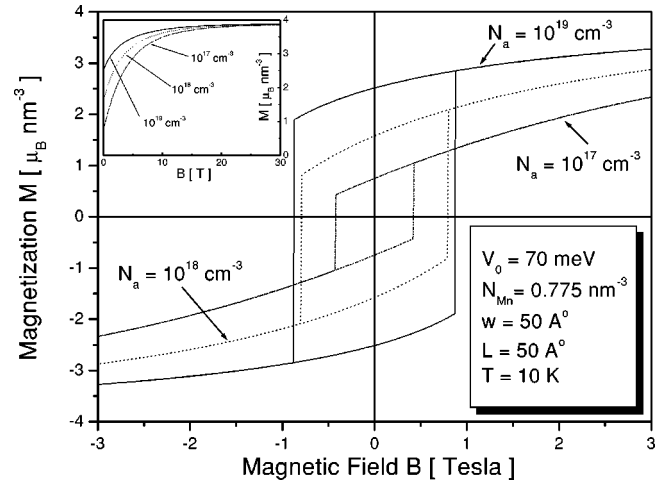


FIG. 3. Magnetic-field dependence of the magnetization of the DMS QW for various impurity-doping concentrations N_a . The inset shows a *paramagnetic* behavior of M beyond a threshold magnetic field B_{th} before it gets saturated.

15% in terms of T_c over the range of the free-carrier concentrations examined.

The exchange and correlations of free carriers increase the spin subband separations of a semiconductor QW structure,⁷ primarily by lowering the subband bottom energies of majority spin states due dominantly to the exchange interaction of the free carriers in the same spin states and hence increasing the spin polarization ζ of the system. The increase in ζ favors the ferromagnetic phase compared to the paramagnetic phase.

The magnetization M of the system is evaluated at finite temperature as a function of magnetic field B and the hysteretic behavior is observed in the DMS QW.¹³ Figure 3 shows the magnetic-field dependence of the magnetization for three different values of doping concentrations of acceptor impurities in the barrier region of the QW. It is clearly seen that the remnant values of M_{rem} increase as the doped impurity concentration N_a and, hence, carrier concentration n_{2D} increase and that M shows *paramagnetic* behavior beyond the threshold magnetic field B_{th} until it gets saturated toward the value $M_s = N_{Mn} g_{Mn} \mu_B S$, the dominating contribution of the localized spins. The inset of the figure shows an asymptotic behavior of the magnetization as one increases the strength of an external magnetic field. Under a high magnetic field $B \geq B_{th}$, a Brillouin function gets saturated to show paramagnetic behavior. The magnitude of B_{th} is sensitive to n_{2D} , N_{Mn} , and the p -doping concentration N_a in nonmagnetic barriers of the DMS quantum structure. The present observation of a hysteretic behavior in M is a direct consequence of the spontaneous spin polarization of the Mn-doped DMS QW structure due to the exchange coupling of a Mn²⁺ ion and an itinerant carrier in the QW.¹⁴ Sharp magnetic hysteresis loops indicate a well-ordered ferromagnetic structure of the QW in agreement of recent experimental observation in a DMS thin film.²

In conclusion, the interplay of the indigenous quantum confinement and magnetic ordering effects is seen to introduce new features to the magnetic phase structure of the

Mn-doped III-V semiconductor quantum well structure. Our result shows hysteretic behavior of the magnetization in a DMS QW in virtue of the coupling between a Mn^{2+} ion and an itinerant carrier. The tendency of ferromagnetic ordering increases as the strength of confinement potential increases and the magnetization of the system is strongly dependent on the concentration of localized Mn^{2+} ions, the free-carrier density n_{2D} , and the geometric and doping profile parameters of the QW. The threshold temperature, below which the system becomes a fully polarized ferromagnetic phase ($\zeta = 1$) spontaneously, increases as one increases the magnetic impurity concentration N_{Mn} in the well and p -doping concentration N_a in nonmagnetic barriers.

The magnetic phase ordering and hysteretic behavior of a Mn-doped DMS QW predicted in the present work would be demonstrated in such experiments as spin-flip light scattering and magnetization measurement with a quantum interference magnetometer. Details of the self-consistent spin subband structure and the quantum well parameter dependence of the magnetic phase structure will be reported in a separate paper.

ACKNOWLEDGMENTS

This work was supported in part by the KOSEF (R02-2000-00047). One of the authors (K.S.Y.) acknowledges J. J. Quinn for useful discussions on the subject.

*Corresponding author. Electronic address: ksyi@pnu.edu

¹See, for example, G. A. Prinz, *Science* **282**, 1660 (1998).

²H. Ohno, *J. Magn. Magn. Mater.* **200**, 110 (1999).

³T. Dietl, A. Haury, and Y. M. d'Aubigné, *Phys. Rev. B* **55**, R3347 (1997).

⁴A. Haury, A. Wasiela, A. Arnoult, J. Cibert, S. Tatarrenko, T. Dietl, and Y. M. d'Aubigné, *Phys. Rev. Lett.* **79**, 511 (1997).

⁵A. B. Oparin and J. J. Quinn, *Solid State Commun.* **98**, 791 (1996).

⁶H. J. P. Freire and J. C. Egues, cond-mat/0112263 (unpublished).

⁷S. P. Hong, K. S. Yi, and J. J. Quinn, *Phys. Rev. B* **61**, 13 745 (2000).

⁸O. Gunnarsson and B. I. Lundqvist, *Phys. Rev. B* **13**, 4274 (1976).

⁹B. Lee, T. Jungwirth, and A. H. MacDonald, *Phys. Rev. B* **61**, 15 606 (2000).

¹⁰L. Brey and F. Guinea, *Phys. Rev. Lett.* **85**, 2384 (2000).

¹¹C. D. Simserides, *J. Phys.: Condens. Matter* **11**, 5131 (1999).

¹²C. Kittel, *Introduction to Solid State Physics* (Wiley, New York, 1996).

¹³N. Kim, S. J. Lee, T. W. Kang, K. S. Yi, and G. Ihm, *J. Korean Phys. Soc.* **39**, 1050 (2001).

¹⁴H. J. Kim, K. S. Yi, N. Kim, S. J. Lee, and J. J. Quinn, *Physica E* **12**, 383 (2002).